SHALLOW WATER SURGE RESISTANCE IDENTIFICATION FOR INLAND VESSELS

Arne Eggers,
Mechanical Engineering Technology Cluster TC, Campus Group T Leuven, KU Leuven, Belgium

Gerben Peeters,
SB PhD fellow at FWO, Faculty of Engineering Technology, KU Leuven, Belgium

Peter Slaets and **Maarten Vanierschot**, Mechanical Engineering Technology Cluster TC, Campus Group T Leuven, KU Leuven, Belgium

SHALLOW WATER SURGE RESISTANCE IDENTIFICATION FOR INLAND VESSELS

Arne Eggers Mechanical Engineering Technology Cluster TC, Campus Group T Leuven, KU Leuven, Belgium
Gerben Peeters, SB PhD fellow at FWO, Faculty of Engineering Technology, KU Leuven, Belgium
Peter Slaets and **Maarten Vanierschot,** Mechanical Engineering Technology Cluster TC, Campus Group T Leuven, KU Leuven, Belgium

SUMMARY

Shifting from classical means of transportation, such as road traffic, towards inland shipping and railway transport is a possible answer to the frequent traffic jams and the high level of pollution on Belgian and European roads. Inland shipping has a comparably low environmental impact, in terms of noise and energy consumption, and might become more economical if the vessels are operating under a high level of autonomy. Model based autonomous sailing algorithms can benefit from the knowledge of the vessel's hydrodynamic behavior. In comparison to seagoing vessels, little to none research has been conducted on how to identify inland ships using computation fluid dynamics (CFD), particularly in shallow water. Hence, this research developed a CFD model to predict the resistance forces acting on inland vessels in shallow water. To proof this methodology, a benchmark vessel for seagoing ships, the KVLCC2 hull, has been examined.

NOMENCLATURE

B	Width of the hull (m)
C_B	Block coefficient (-)
Co	Courant Number (-)
Co_{FS}	Courant Number in the free surface (-)
t	Time (s)
T	Draft of the hull (m)
T_{ij}	Viscous stress (Pa)
L_{pp}	Length between perpendiculars of the Hull (m)
g_i	Gravitational constant i=1-3 (m/s^2)
h	Height field (m)
$\bar{p}'$	Time averaged gravity corrected pressure (N/m^2)
$\bar{u}_i$	Time averaged velocity i = 1-3 (m/s)
$\overline{u_i u_j}$	Reynolds stress tensor i,j = 1-3 (Pa)
u_{main}	Ship velocity (m/s)
u^+	Non-dimensional velocity (-)
U	Uncertainty of CFD values (N)
UKC	Under keel clearance (%)
r	Grid refinement ratio (-)
R	Grid convergence ratio (-)
y^+	Non-dimensional wall distance (-)
x_i	Spatial coordinate i = 1-3 (m)
X	Drag Force (N)
ϵ	Difference between CFD and EFD Values (%)
ϵ_{ij}	Difference between grid i and grid j Values (%)
ΔX	Difference in drag force between grids (N)
λ	Scaling factor (-)
μ	Viscosity of mixture (Pa s)
μ_{air}	Viscosity of air (Pa s)
μ_{water}	Viscosity of water (Pa s)
ρ	Density of mixture (kg/m^3)
ρ_{air}	Density of air (kg/m^3)
ρ_{water}	Density of water (kg/m^3)
ϕ	VoF scalar (-)

1 INTRODUCTION

The growing demand for mobility and transportation in the European Union and the world, leads to the development of new concepts and ideas in the transportation sector. As the massive personal and freight transport on roads introduces traffic jams, accidents and pollution, a shift towards a more balanced transportation concept, including railway transport and inland shipping, is natural. As its energy consumption per km/ton is roughly 17% of that of road and 50% of that of railway transport, the environmental impact of inland shipping is considered to be small (European Commission, 2018). Therefore, it is an important part of the European transportation network. However, due to the relatively high need of labor and the tough competition on the transportation market, it is at the moment mostly economical by deploying huge ships with high loading capacities. These larger barges are in many cases only suited for entering deeper channel systems. The more shallow or confined regions, which are often apparent in northern Europe, need to be fed by smaller barges. To serve this need, the European Watertruck+ project aims to build medium and small sized vessels of the European Class (CEMT) type ranging from I to IV ("Watertruck+," 2018). These vessels are applied in modular designed convoys, consisting of self-propelled, non-propelled and push ships, which increases the economic and technical flexibility. A possibility to further improve the economic competitiveness of the CEMT barges is to make them autonomous or semi-autonomous, thus decreasing the need of manual labor. Identification of the hydrodynamic characteristics for these vessels is a necessity to improve modern control algorithms for autonomous sailing ships.
The state-of-the-art measures to identify ship characteristics may be separated into three groups. Firstly, a scale model may be investigated by measuring the forces acting on it in a towing tank by applying experimental fluid dynamic (EFD) (G. Delefortrie, K. Eloot, & F. Mostaert, 2013). EFD applications suffer from the relatively high costs of building a scale model or a real size ship and the

need of a towing tank. This makes it difficult to apply EFD in the early design stage of a vessel to optimize its shape. However, EFD values based on scale models may be scaled to the real size vessel and are known to be very reliable and accurate. Hence, they are often applied as validation proving the methodology of other cheaper methods right. Secondly, regression formulae, which combine different data sets of comparable cases to calculate the best fitting coefficient, may be used (Hans and Zhao, 2017). The method is computationally cheap and produces fast results. Nevertheless, if the available data for the investigated hull is limited or the influence of geometrical changes should be assessed this method becomes difficult to apply reasonably. Thirdly, CFD may be applied to solve the governing physical equations numerically. As such, the geometry is represented by a numerical grid which is able to capture the relevant features. Thus, influences of geometrical changes and other parameters may be predicted. The generated data can also be used to optimize the hydrodynamic shape of the current inland vessels (Rotteveel, Hekkenberg, & van der Ploeg, 2017). However, CFD methodologies are often complex combinations of different state-of-the-art models, performing differently depending on the actual physics involved and the exact set up. Hence, applied CFD has to be validated by data usually based on EFD results where the validation case has to feature the same physical phenomena as the actual identification case.

Ship hulls may be mainly divided into two field of application, inland and seagoing vessels. The latter have been subject of EFD and CFD studies frequently (Guo & Steen, 2011)(SIMMAN, 2014). Benchmarks hulls such as the KVLCC2 or DTC hull have been investigated numerically in open water conducting manoeuvres, such as zig-zag or turning circles (Shigunov, el Moctar, Papanikolaou, Potthoff, & Liu, 2018), in shallow water (Toxopeus, 2013) and in waves (Guo & Steen, 2011). However, only little research has been conducted on the identification inland vessels in general and on the smaller CEMT I and II types, particularly (Rotteveel et al., 2017). This is especially true for shallow water simulations, although inland vessels are facing shallow and restricted water not only in harbors or during docking manoeuvres but most of the time in channels and rivers. Hence, methodologies which predict the flow around CEMT type vessels in open and shallow waters are a necessity to accelerate the optimization of future vessel generations and to enable the development of more automated and autonomous inland vessels.

To close this literature gap, this research developed a CFD based model to identify inland vessels in shallow water. The inland vessel is the CEMT I, which is a basic self-propelled barge of the CEMT type with a high block coefficient ($C_B = 0.95$). As there is little to no EFD data on inland vessels available this research validates its methodology based on the KVLCC2 hull. As stated earlier, plenty of EFD and CFD data on this hull in various conditions are available. Additionally, the KVLCC2 hull features a rather high block coefficient ($C_B = 0.81$) which is close to the usual values of inland ships. However, the KVLCC2 hull is shaped more hydrodynamical, preventing flow detachment, which will most probably occur on the CEMT I's block shaped hull. This might give rise to transient behavior. Furthermore, the KVLCC2 hull is designed to bear an external propeller, while the CEMT I hull features an internal actuation. As it has no external actuation, CEMT I bare hull simulations are expected to show higher alignment with the in-operation flow fields of the vessel. The open source toolbox OpenFOAM (OpenCFD, 2018) solves the governing equations in the computational domain, which is discretized using a hexahedron dominant mesh generated with the open source mesh generation software snappyHexMesh. The turbulent fluctuations were modelled by the frequently applied k-omega SST turbulence model (Menter, 1994). As the wave pattern influences the hull's resistance force the free surface needs to be taken into account. Here, a Volume of Fluid (VoF) method (Hirt & Nichols, 1981) is applied. This paper continues with chapter 2 describing the applied methodology, chapter 3 discussing the results and chapter 4 draws a conclusion.

2 METHODOLOGY

2.1 FLOW MODELING

OpenFOAM solves the Reynolds averaged Navier-Stokes(RANS) equations:

$$\frac{\partial \bar{u}_i}{\partial x_i} = 0, \tag{1}$$

$$\frac{\partial \bar{u}_i}{\partial t} + \bar{u}_j \frac{\partial \bar{u}_i}{\partial x_j} = \frac{1}{\rho}\frac{\partial \bar{p}}{\partial x_i} + \frac{\partial}{\partial x_i}\left(\frac{1}{\rho}T_{ij} - \overline{u_i{}' u_j{}'}\right) + g_i. \tag{2}$$

Where $\bar{u}_i$ is the time averaged velocity, t is the time, x_i the spatial coordinate, $\bar{p}$ the time averaged pressure, T_{ij} the viscous stresses, $\overline{u_i{}' u_j{}'}$ the Reynolds stresses and g_i the gravitational constant. In the RANS equations the turbulent fluctuations are time averaged to reduce the computational costs. Therefore, the mean flow has to be modelled. This is done by applying the k-omega SST turbulence model, which combines the higher stability of the k-epsilon model with the better wall flow and separation prediction of the original k-omega model. The free surface is modelled by a VoF method which establishes a scalar function ϕ. This function indicates which phase is apparent in a fluid cell, where $\phi = 0$ indicates the presence of air, $\phi = 1$ of water and $0 < \phi < 1$ of the free surface between the two phases. The scalar function is transported passively with the predicted flow field:

$$\frac{\partial \phi}{\partial t} + \bar{u}_j \frac{\partial \phi}{\partial x_j} = 0. \tag{3}$$

Once the flow field and the phase distribution is known the scalar function ϕ may be applied to determine the local flow properties:

$$\rho = \phi \rho_{water} + (1 - \phi)\rho_{air}, \tag{4}$$

$$\mu = \phi \mu_{water} + (1 - \phi)\mu_{air}. \tag{5}$$

Where ρ is the mixture density, ρ_{water} the water density, ρ_{air} the air density, μ the mixture viscosity, μ_{water} the water viscosity and μ_{air} the air viscosity. The no slip wall boundary conditions in these simulations are handled by the law of the wall, formulated by Spalding in 1961 (Spalding, 1961). This approach computes the velocity in the first grid cell at the wall based on a law which fits experimental data for universal turbulent flows over the complete boundary layer ranging from $y^+ = 0$ to $y^+ = 300$:

$$y^+ = u^+ + 0.1108 \cdot \left(e^{0.4u^+} - 1 - 0.4u^+ - \frac{(0.4u^+)^2}{2!} - \frac{(0.4u^+)^3}{3!}\right). \quad (6)$$

Where u^+ is the non-dimensional velocity and y^+ the non-dimensional wall distance. In comparison to classical wall functions, this approach offers more flexibility and accuracy as also grid points within the viscous sublayer and the buffer layer can be handled and a higher resolution of the boundary layer automatically leads to a more grid independent solution. However, it still benefits from the advantages of wall functions, such as lower cell count and higher convergence rate in the wall boundary layers.

2.2 VESSELS

The methodology is validated by the frequently examined KVLCC2 hull, which combines a high block coefficient ($C_B = 0.81$) with publicly available EFD data for shallow and free water cases. In table 1, where L_{pp} is the length between perpendiculars, B the width, T the draft, C_B the block coefficient and λ the scaling factor, the characteristics of the different vessel are compared. The two hulls show similarities in all characteristics which leads to comparable Froude and Reynolds numbers at the same longitudinal velocities. Figure 1 shows the KVLCC2 and CEMT I hulls in side and top view. As the KVLCC2 hull is a seagoing tanker, its shape is optimized to minimize hydrodynamic resistance forces. Whereas, the primary design goal of the CEMT I is a maximum of payload while keeping the hull's production cost low. Therefore, the block coefficient of the CEMT I is higher and the hull shape features sharp corners which may introduce detachment.

Table 1. Vessel Characteristics

	CEMT I		KVLCC2	
	full size	scale model	full size	scale model
$L_{pp}\ (m)$	38.5	4.81	320	4.27
$B\ (m)$	5.05	0.63	58	0.77
$T\ (m)$	1.8	0.23	20.8	0.28
C_B	0.95	0.95	0.81	0.81
λ	1	8^{-1}	1	75^{-1}

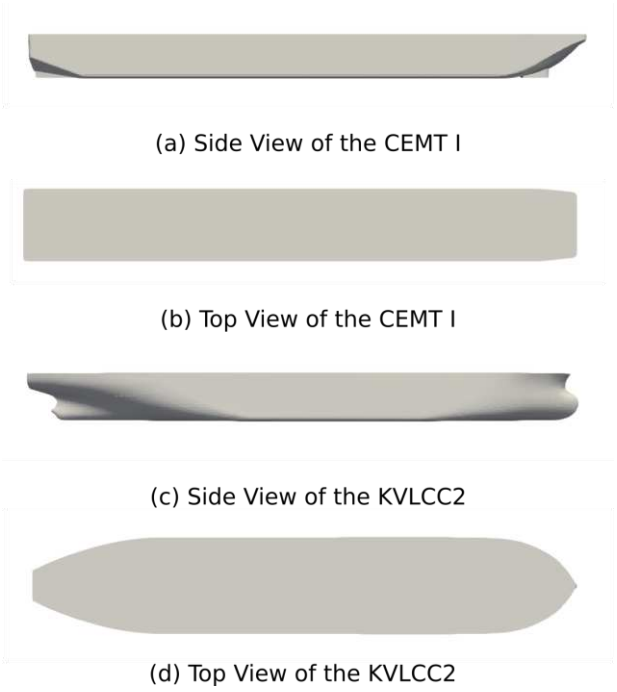

Figure 1. Investigated ship hulls

2.3 CASE SETUP

As no or only minimal transient behavior was observed in transient simulations, all cases converge towards a steady state, which was assumed to be reached if the fluctuations of the drag force drop under a tolerance value. This steady state was achieved in a stable and efficient way by local time stepping (LTS), allowing spatial variations of the time step, only limited by the maximum local Courant number, which is defined by the user for the single phase and the free surface areas differently. This approach allows to separate the time scales around the free surface from the rest of the domain (Jasak, Vukčević, & Christ, 2014). These methods have been applied to seagoing vessels, incorporating different modifications to the algorithm, and are known to be comparable to commercial software in terms of efficiency and robustness (Kim & Park, 2017). The maximum local Courant number was set to Co = 1000 during most of the computations, only reduced to Co = 1 to minimize fluctuations and inaccuracy when determining the final value, while the free surface Courant number was kept at $Co_{FS} = 1$ to assure convergence of the free surface flow. A second order upwind scheme handles the convective term for momentum and a van Leer limited TVD-Scheme the VoF scalar. The LTS scheme implemented in OpenFOAM applies a first order Euler discretization to the time derivatives, which is sufficient as transient behavior is not studied. The computational domain is set up around a body fixed coordinate system. The domain and the physical boundary conditions are depicted in figure 2, where u_{main} is the inlet velocity. Here, the wall velocities of the no slip walls, the hull and the bottom patch, are described. Based on these the velocities in the cells at the wall are set according to equation 6.

The pressure on all walls and the inlet is set by applying a body force corrected zero gradient boundary condition.

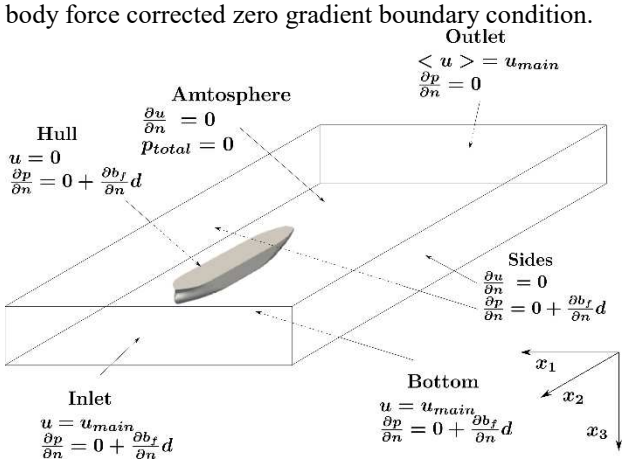

Figure 2. Case setup and boundary conditions

To increase the solver's convergence rate the outlet velocities are set to values which average to u_{main}, together with the imposed inlet velocity this assures conservation of mass for the water phase, over the whole domain. The shallow water setup is described in figure 3, the side walls are placed in sufficient distance to assume their influence neglectable. The bottom is placed based on the experimental data available for the KVLCC2 hull to generate shallow water conditions at 20% and 50% under keel clearance (UKC), while the investigated velocities are orientated at the allowed maximum in local Belgium channel systems ("VisuRIS - Kanaal Leuven-Dijle," 2018).

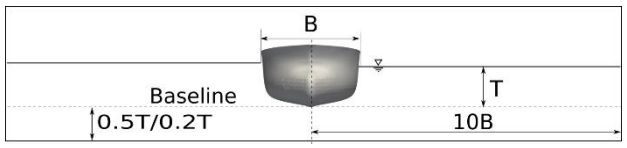

Figure 3. Geometrical shallow water setup

2.4 GRID STUDY

The hexahedra dominated computational meshes were generated by the open source software snappyHexMesh. The cells are clustered around the hull applying six refinement boxes, each of them decreasing the characteristic cell size by factor two. At the no slip boundary conditions, boundary layer cells have been added to resolve the physical boundary layer. An example for the KVLCC2 hull is shown in figure 4. The grid independence study has been conducted for the K50 test case, which is described in table 4, and the grid sizes are described in table 2.

Table 2. Grid characteristics

	coarse	medium	fine
number	3	2	1
cells x10^6	0.78	2.43	6.81

According to the International Towing Tank Conference's guideline the refinement ratio between the different grids in all spatial dimension was set onto a value close to $r = \sqrt{2}$ (ITTC, 2017). The differences between the computations on the grids are shown in table 3. The grid convergence ratio can be calculated:

$$\mathrm{R} = \frac{\epsilon_{1,2}}{\epsilon_{3,2}}. \quad (7)$$

Where R is the grid convergence ratio and ϵ_{ij} the error percentage between grid i and j. As depicted in figure 5, where X is the predicted drag force and ΔX is the difference between the computed drag forces on different grids, the grid convergence is oscillatory and the uncertainties may be estimated:

$$U = \frac{X_{max} - X_{min}}{2}. \quad (8)$$

Where U is the uncertainty and X_{max} and X_{min} the maximum and minimum drag forces predicted on different grids.

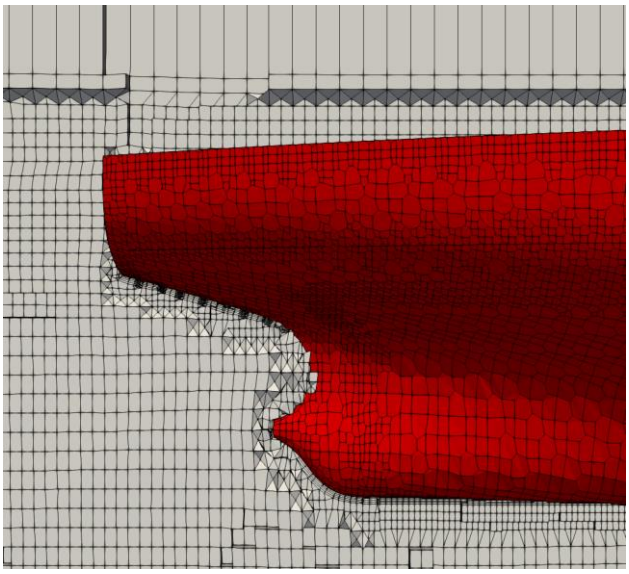

Figure 4. Computational Mesh around the stern of the KVLCC2

The EFD's uncertainty of 0.06N on a 68% confidence interval is in the same order of magnitude as the oscillation of the simulations on different numerical grids (G. Delefortrie et al., 2013). Hence, it may be seen as sufficiently small. The medium grid was selected for the following simulations as it (i) made simulations with reasonable computational costs possible and (ii) featured a low uncertainty based on the conducted grid study.

Table 3. Grid study

	3 to 2	2 to 1
r	1.46	1.41
$\Delta X\ (N)$	0.16	-0.14
$\epsilon(\%)$	5.2	-4.8

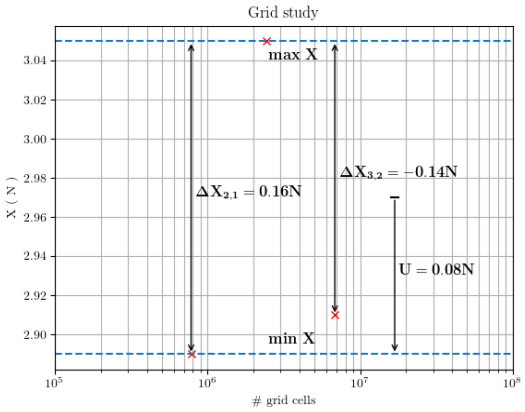

Figure 5. Oscillating grid convergence. Grid convergence Ratio R = -0.92

3 RESULTS

3.1 CFD EFD KVLCC2

Table 4. Test case characteristics, CFD results and error compared to EFD values

	u_{main}	UKC	hull	X (N)	ϵ(%)
K50	0.416	50%	KVLCC2	3.05	-1.4
K20	0.416	20%	KVLCC2	3.6	-0.55
C2.50	0.2	50%	CEMTI	1.31	-
C4.50	0.4	50%	CEMTI	3.96	-
C2.20	0.2	20%	CEMTI	1.7	-
C4.20	0.4	20%	CEMTI	4.4	-

Even though the hull was assumed to be fixed and no sinkage or trim was taken into account, the drag forces could be predicted with a maximum error of $\epsilon = -1.4\%$ for the relevant velocities. Furthermore, all simulations underestimate the drag which is reasonably as the actual sinkage and trim in EFD are increasing the drag force. The computed drag forces for the KVLCC2 and CEMT I hulls are listed in table 4. The values of the KVLCC2 hull are compared to EFD values to validate the methodology. In figure 6 the gravity corrected pressure fields around the KVLCC2 hull is depicted at 50% and 20% UKC. The gravity corrected pressure is defined as the static pressure without the gravity component:

$$\bar{p}' = \bar{p} - \rho g_i h. \tag{9}$$

Where $\bar{p}'$ is the time averaged gravity corrected pressure and h the height field. Removing the gravity component from the pressure field increases the visibility of effects occurring due to ship and wave dynamics as in hydrodynamic applications these are often small compared to gravity. Furthermore, the pressure iso-lines in figure 6 are computed using only the hexahedral cells, as the polygons in the free surface influence the pressure strongly. However, the influence on the wave pattern was found not to have a strong influence on the computed drag, as the results match experimental data. The area under the hull is reduced due to the shallowness of the set-up, introducing a higher resistance. Thus, the pressure at the bow is increased leading to a higher pressure drag. Furthermore, the smaller cross section forces higher velocities below the vessel, increasing the viscous drag component. Both of these effects amplify by lowering the UKC value.

3.2 CFD CEMT I

After validating the methodology on the KVLCC2 hull it could be used to predict the drag forces acting on the CEMT I at multiple velocities. As such, this data was applied to identify the coefficients of the second order single variable polynomial fit for the CEMT I hull:

$$X = X_u u_{main} + X_{uu} u_{main}^2. \tag{10}$$

Where X_U and X_{UU} are the linear and quadratic coefficient. Table 4 shows the drag forces on the CEMT I hull. Due to the same effects described for the KVLCC2 hull, the drag increases while reducing the UKC. Figure 6 compares the surface flow field for the CEMT I and the KVLCC2 hull. Due to the less hydrodynamic shape of the CEMT I hull the flow detaches at the stern creating a low pressure zone, increasing the pressure drag. This becomes visible as well in the comparison of the pressure in the symmetry plane. At the stern of the KVLLC2 hull only little detachment is occurring. Hence, the pressure remains high, while the CEMT I creates a low pressure wake over the full draft of the hull. This implies massive potential for improvement of the CEMT I's shape. However, other constraints such easy manufacturing and high pay load have to be taken into account. To assess the possibility of transient effects due to vortex shedding in the CEMT I's wake, transient simulation have been conducted for the C4.50 and C4.20 cases. Nevertheless, no or only minimal transient effects have been observed.
Figure 7 shows the CEMT I's polynomial fits for different UKCs and open water. These may be used to build control algorithms for the CEMT I.

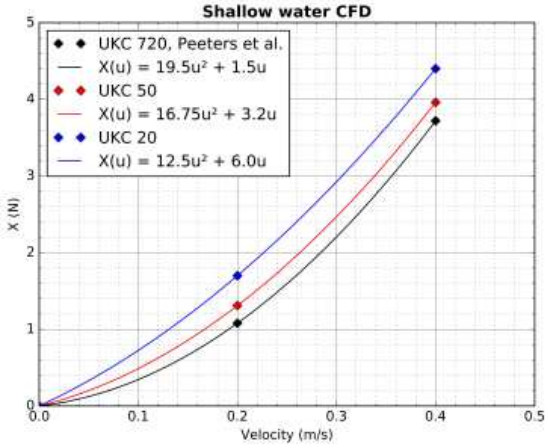

Figure 7. Polynomial fit for the drag forces of the CEMT I hull at different UKCs. UKC 720 values from (Peeters, Eggers, Boonen, Slaets, & Vanierschot, 2018)

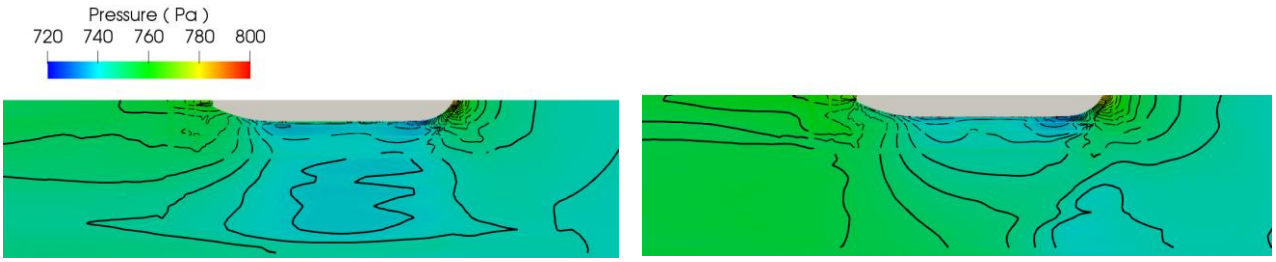

(a) Relative gravity corrected pressure around the KVLCC2 hull at 50% UKC (left), 20% UKC (right) and $u_{main} = 0.416m/s$

(b) Relative gravity corrected pressure around the CEMT I hull at 50% UKC (left), 20% UKC (right) and $u_{main} = 0.4m/s$

(c) Relative gravity corrected pressure around the KVLCC2 hull at 50% UKC and $u_{main} = 0.416m/s$

(d) Relative gravity corrected pressure around the KVLCC2 hull at 20% UKC and $u_{main} = 0.416m/s$

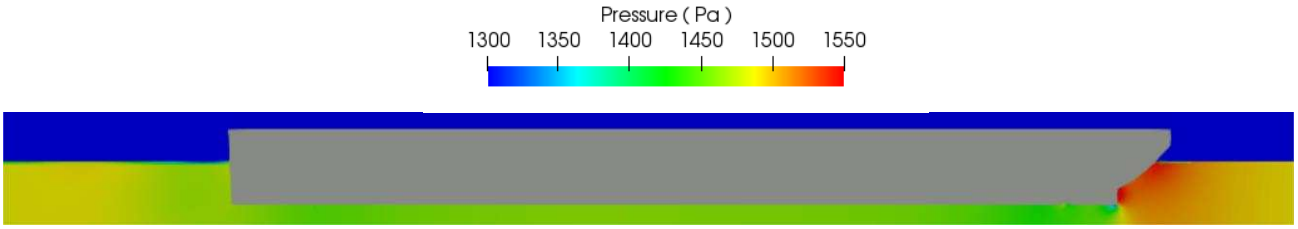

(e) Relative gravity corrected pressure around the CEMT I hull at 50% UKC and $u_{main} = 0.4m/s$

(f) Relative gravity corrected pressure around the CEMT I hull at 20% UKC and $u_{main} = 0.4m/s$

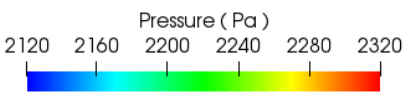

Figure 6. Comparison of relative gravity corrected pressure around the CEMT I and KVLCC2 hull

4 CONCLUSION

OpenFOAM's VoF solver in combination with the LTS scheme offers a robust and efficient tool to predict drag forces on ship hulls with high block coefficients in shallow water. The applied methodology was proven to be working on the KVLCC2 benchmark case. Furthermore, the CEMT I hull got investigated and the derived drag forces were used to identify the coefficients of the second order single variable polynomial fit for the CEMT I hull. This can be used in future research to create algorithms increasing the level of autonomy of the CEMT I ships.

5 ACKNOWLEDGEMNT

The computational resources and services used in this work were provided by the VSC (Flemish Supercomputer Center), funded by the Research Foundation - Flanders (FWO) and the Flemish Government – department EWI. The authors would also like to thank the FWO for funding the research of G. Peeters, project 1S12519N.

6 REFERENCES

European Commission, 2018. Inland waterways - Mobility and Transport - European Commission. Retrieved from /transport/modes/inland_en

Delefortrie, G, Eloot, K., Mostaert, F., 2013. *Execution of Model Tests with KCS and KVLCC2. Version 3_0. WL Rapporten, 00_066*. Flanders Hydraulic Research Antwerp, Belgim.

Guo, B., Steen, S., 2011. Evaluation of added resistance of kvlcc2 in short waves. *Journal of Hydrodynamics, Ser. B*, *23*(6), 709–722. https://doi.org/10.1016/S1001-6058(10)60168-0

Hirt, C. W., Nichols, B. D. , 1981. Volume of fluid (VOF) method for the dynamics of free boundaries. *Journal of Computational Physics*, *39*(1), 201–225. https://doi.org/10.1016/0021-9991(81)90145-5

ITTC, 2017. Uncterainty Analysis in CFD Verification and Validation Methodology and Procedures. Retrieved from: https://www.ittc.info/media/8153/75-03-01-01.pdf

Jasak, H., Vukčević, V., Christ, D., 2014. Rapid Free Surface Simulation for Steady-State Hull Resistance with FVM using OpenFOAM. In *30 Symposium on Naval Hydrodynamics*. Retrieved from: http://bib.irb.hr/datoteka/727067.SteadyNavalHydroSolver002.pdf

Kim, G.-H., Park, S., 2017. Development of a numerical simulation tool for efficient and robust prediction of ship resistance. *International Journal of Naval Architecture and Ocean Engineering*, *9*(5), 537–551. https://doi.org/10.1016/j.ijnaoe.2017.01.003

Liu, J., Hekkenberg, R., Quadvlieg, F., Hopman, H. Zhao, B., 2017. An integrated empirical manoeuvring model for inland vessels. *Ocean Engineering*, *137*, 287–308.

Menter, F. R., 1994. Two-equation eddy-viscosity turbulence models for engineering applications. *AIAA Journal*, *32*(8), 1598–1605. https://doi.org/10.2514/3.12149

OpenCFD, 2018. OpenFOAM® - Official home of The Open Source Computational Fluid Dynamics (CFD) Toolbox. Retrieved on 11/10/2018 from http://www.openfoam.com

Peeters, G., Eggers, A., Boonen, R., Slaets, P., Vanierschot, M., 2018. Surge resistance identification of inland vessels by computational fluid dynamics. In *2018 OCEANS - MTS/IEEE Kobe Techno-Oceans, OCEANS - Kobe 2018*. https://doi.org/10.1109/OCEANSKOBE.2018.8559048

Rotteveel, E., Hekkenberg, R., van der Ploeg, A., 2017. Inland ship stern optimization in shallow water. *Ocean Engineering*, *141*, 555–569. https://doi.org/10.1016/j.oceaneng.2017.06.028

Shigunov, V., el Moctar, O., Papanikolaou, A., Potthoff, R., Liu, S., 2018. International benchmark study on numerical simulation methods for prediction of manoeuvrability of ships in waves. *Ocean Engineering*, *165*, 365–385. https://doi.org/10.1016/j.oceaneng.2018.07.031

SIMMAN, 2014. Retrieved from https://simman2014.dk/

Spalding, D. B., 1961. A Single Formula for the "Law of the Wall." *Journal of Applied Mechanics*, *28*(3), 455–458. https://doi.org/10.1115/1.3641728

Toxopeus, S. L., 2013. Viscous-Flow Calculations for KVLCC2 in Deep and Shallow Water. In L. Eça, E. Oñate, J. García-Espinosa, T. Kvamsdal, & P. Bergan (Eds.), *MARINE 2011, IV International Conference on Computational Methods in Marine Engineering* (Vol. 29, pp. 151–169). Dordrecht: Springer Netherlands. Retrieved from: http://link.springer.com/10.1007/978-94-007-6143-8_9

VisuRIS - Kanaal Leuven-Dijle, 2018. Retrieved on 22/11/2018 from https://www.visuris.be/Leuven-Dijle

Watertruck+. (2018). Retrieved from http://www.watertruckplus.eu

7 AUTHORS BIOGRAFIES

Arne Eggers is a graduate student at the KU Leuven since 2016. Mr. Eggers specializes in CFD for applied hydrodynamics and aerodynamics. Among other projects, he conducted optimization studies of flow based recycling machines, predictions of the hydrodynamic drag on ships,

and aerodynamic drag on cars. Before starting at the KU Leuven, he completed his master's degree in Computational Engineering at the Technical University of Darmstadt. After that, he worked as a researcher in combustion modeling at the Institute for Energy and Power Plants at the Technical University of Darmstadt.

Gerben Peeters is an SB PhD fellow at FWO (Flanders research foundation). He has been conducting research at the Department of Mechanical Engineering of the KU Leuven since December 2015. His interests lie in the fields of mathematical modelling, identification procedures, and control theory. He combines these interest fields in his doctoral study "Towards Autonomous Inland Shipping" which started in January 2017.

Peter Slaets is a professor at KU Leuven in the area of autonomous mobile robotics with a special focus on inland waterway transport and service robots. After finishing his PhD at KU Leuven, department of Mechanical Engineering in 2008, he joined the electromechanical department at Group T university college in Leuven. At campus Group T, he co-founded the intelligent mobility research group covering both technological and managerial aspects. The integration of campus Group T in KU Leuven in 2013 led to a cross-pollination of engineering technology with engineering leading to new opportunities. Currently he is supervising 6 PhD students and coordinator of several research/industrial projects within the domain of autonomous vehicles with a special focus on inland barges. His long term vision is to transform the Flemish waterways (again) to a competitive and sustainable logistic platform that serve as a viable alternative for road transport.

Maarten Vanierschot is a professor at KU Leuven, campus Group T Leuven. He received a Master's degree in Electromechanical Engineering from the KU Leuven, Belgium in 2002 where he also received a PhD in 2007. He obtained a post-doc scholarship from 2007 till 2009, after which, he became an assistant professor at campus Group T. His research focusses on experimental, numerical and theoretical fluid mechanics with an emphasis on large industrial applications including aerodynamics, hydrodynamics and heat- and mass transfer.